Geochemistry Geophysics Geosystems

Supporting Information for

Deep hydrography of the South China Sea and deep water circulation in the Pacific since the last glacial maximum

Sui WAN[1,2], Zhimin JIAN[2,*], Haowen DANG[2]

1. CAS Key Laboratory of Ocean and Marginal Sea Geology, South China Sea Institute of Oceanology, Chinese Academy of Sciences, Guangzhou, China
2. State Key Laboratory of Marine Geology, Tongji University, Shanghai, China

Contents of this file

Introduction:

This file includes one paragraph text, two tables and four figures supporting the main article.

Table S1: New stable isotopic records of *C. wuellerstorfi* from down-core sediments in the SCS for the late Holocene and the LGM.

Table S2: Stable isotopic records in selected cores from the Southern Ocean and southwest Pacific, western equatorial Pacific, off-Japan margin.

Text S1: Information regarding the determination of the late Holocene and LGM time slices for the down-cores in the SCS.

Figure S1: Age models based on *Globigerinoides ruber* AMS ^{14}C and *C. wuellerstorfi* δ^{18}O of Cores MD05-2904, MD05-2896, MD12-3428, MD12-3433, MD12-3434, SO50-31KL, and MD97-2151 in the SCS.

Figure S2: Determination of the late Holocene and LGM time slices for the *C. wuellerstorfi* δ^{18}O of Cores MD05-2899, SO50-37KL, and SO50-29KL in the SCS.

Figure S3: *C. wuellerstorfi* δ^{13}C records from Cores MD05-2904, MD05-2896, MD12-3428, MD12-3433, MD12-3434, SO50-31KL, and MD97-2151.

Figure S4: *C. wuellerstorfi* δ^{13}C records from Cores MD05-2899, SO50-37KL, and SO50-29KL.

Figure S5: The selected transects in the western and eastern Pacific.

References

Table S1

Core	Date	Sediment Depth (cm)	$\delta^{18}O$ (‰)	$\delta^{13}C$ (‰)
MD12-3428 (20.14N, 115.83E; water depth of 890 m)	Late Holocene (0-6 ky BP)	2	2.11	0.55
		8	1.94	0.57
		14	2.08	0.53
		24	1.91	0.59
		34	2.09	0.55
		44	1.98	0.49
	LGM	234	3.25	0.29
		248	3.24	0.36
		264	3.26	0.24
		276	3.43	0.30
		288	3.30	0.23
MD12-3434 (18.83N, 116.32E; water depth of 2990 m)	Late Holocene	0	2.73	0.17
		4	2.57	0.21
	LGM	156	4.14	0.37
		160	4.06	0.27
		168	4.26	0.35
		172	4.28	0.34
		176	4.07	0.39
		180	4.09	0.36
		184	4.08	0.39
		192	4.12	0.30
		208	4.04	0.25
MD12-3433 (19.28N, 116.24E; water depth of 2125 m)	Late Holocene	2	2.51	0.36
		4	2.58	0.31
		10	2.73	0.38
		14	2.58	0.42
		20	2.71	0.41
	LGM	196	4.05	-0.87
		206	4.07	-0.36
		216	4.19	0.16
		226	4.17	-0.39
		238	3.94	-0.39
		244	4.04	-0.37
		250	4.06	-0.26
		254	4.17	-0.30
		264	4.19	-0.24
		298	3.80	-0.23
		304	4.16	-0.09
		306	4.23	-0.23
		312	4.00	-0.47

37

Core	Date	Sediment Depth (cm)	$\delta^{18}O$ (‰)	$\delta^{13}C$ (‰)
MD05-2899 (13.79N, 112.18E; water depth of 2393 m)	Late Holocene	3	2.56	0.25
		5	2.75	0.30
		7	2.45	0.21
		9	2.59	0.27
		11	2.62	0.24
		13	2.65	0.26
		15	2.61	0.24
		17	2.68	0.26
	LGM	63	4.23	-0.13
		65	4.19	-0.19
		67	4.11	-0.12
		69	4.09	-0.24
		71	3.98	-0.10
		73	4.14	-0.19
		75	4.00	-0.17
		77	4.11	-0.09
		79	3.93	-0.19
		81	3.99	-0.13
		83	3.94	-0.05
		85	3.84	-0.21
MD05-2896 (8.83N, 111.44E; water depth of 1657 m)	Late Holocene	1	2.66	0.19
		9	2.61	0.30
		17	2.59	0.21
	LGM	145	4.16	-0.03
		150	4.09	-0.21
		156	4.09	-0.07
		162	4.04	-0.19
		170	3.92	-0.23
		174	3.92	-0.19
		178	3.97	-0.17
		182	3.91	-0.17
		186	4.03	-0.18
		190	3.78	-0.20
		194	4.08	-0.14
		198	3.97	-0.05
		202	3.96	-0.16
		206	3.95	-0.14

38

39

40

Core	Date	Sediment Depth (cm)	$\delta^{18}O$ (‰)	$\delta^{13}C$ (‰)
MD05-2904 (19.46N, 116.15E; water depth of 2066 m)	Late Holocene	1	2.67	0.30
		9	2.76	0.33
		15	2.60	0.36
		25	2.81	0.46
		29	2.76	0.17
		33	2.67	0.30
		43	2.59	0.32
		49	2.75	0.33
		57	2.67	0.37
	LGM	665	4.08	-0.31
		711	3.92	-0.43
		744	3.89	-0.24
		757	4.00	-0.31
		769	3.95	-0.31
		809	3.81	-0.51
		849	3.81	-0.27
		866	3.83	-0.14
		907	3.94	-0.30

41

42

43 **Table S2**

Core	Lat. (N)	Long. (E)	w.d. (m)	$\delta^{18}O$ Hol.	$\delta^{13}C$ Hol.	$\delta^{18}O$ LGM	$\delta^{13}C$ LGM	Reference
ERDC92bx	-2.22	156.98	1622	2.40	0.41	3.73	0.21	Herguera et al., [1992]
ERDC88bx	0.03	155.87	1933	2.46	0.42	3.8	0.03	
ERDC113p	-1.63	159.22	2157	2.61	0.31	4.07	-0.08	
ERDC112bx	-1.62	159.23	2170	2.65	0.39	4.08	-0.02	
ERDC120bx	-0.02	158.68	2257	2.58	0.40	3.9	-0.08	
ERDC83bx	1.4	157.3	2357	2.72	0.40	4.04	-0.02	
ERDC79bx	2.78	156.22	2780	2.58	0.40	4.12	-0.07	
ERDC123bx	-0.02	160.4	2943	2.72	0.33	4.06	-0.10	
ERDC125bx	0	160.98	3379	2.66	0.35	4.14	-0.17	
ERDC108bx	-1.73	160.8	3403	2.69	0.31	4.16	-0.12	
ERDC135bx	0.87	160.98	3503	2.78	0.38	4.15	-0.02	
ERDC77bx	4.85	156.05	3591	2.67	0.22	4.14	-0.14	
ERDC128bx	0	161.42	3740	2.79	0.29	4.07	-0.12	
ERDC136bx	1.1	161.6	3852	2.88	0.33	4.23	0.02	
ERDC139bx	1.35	162.38	4164	2.97	0.40	4.06	-0.02	
ERDC129bx	0	161.97	4127	2.89	0.36	4.18	0.06	
ERDC131bx	-0.02	162.7	4438	2.87	0.48	4.12	-0.03	
KH82-4-14	31.44	129.02	740	——	——	2.68	0.38	Matsumoto et al., [2002]
PN3PC	28.06	127.55	1058	2.25	0.07	3.35	0.11	
V20-133	32.58	140.34	1503	2.69	−0.07	3.85	-0.19	
V28-297	31.59	140.26	2047	——	——	3.91	-0.14	
MR97-4	35.59	141.48	2308	2.69	0.1	4.11	——	
KT89-18 P4	32.09	133.54	2700	2.40	−0.12	4.52	-0.2	
PC14	32.4	138.27	3252	2.83	0.34	4.08	-0.09	
PC16	31.55	138.25	3320	2.83	0.51	4.26	-0.07	
RS67-GC27	38.648	141.192	506	1.03	1.55	2.85	1.91	Bostock et al., [2013] and therein
RS78-GC18	41.385	144.233	814	1.44	1.13	3.11	1.20	
SO36-SL17	42.052	144.585	1042	2.01	1.04	3.13	0.84	
DSDP 594	45.524	174.948	1204	2.88	1.16	4.49	0.06	
MD97 2120	45.534	174.931	1210	2.67	0.90	4.38	0.32	
CHAT 16K	42.533	-1.5	1408	2.42	0.96	3.96	0.43	
P69 (PC)	40.397	177.997	2197	2.93	0.45	4.61	-0.32	
MD97 2121	40.38	177.99	2314	2.99	0.39	4.56	-0.37	
RS67-GC13	38.465	140.167	2525	2.46	0.55	4.18	-0.22	
CHAT 10K	40.033	179.997	3003	2.95	0.67	4.49	-0.73	
ODP 1123	41.786	-8.5	3290	2.94	0.54	4.50	-0.52	
CHAT 1K	41.583	-8.5	3556	2.68	0.71	4.18	-0.22	
CHAT 5K	40.783	-8.45	4240	2.65	0.45	4.26	-0.38	
CHAT 3K	42.658	-12.5	4802	2.62	0.36	4.25	-0.34	

44

Text S1

The chronological constraints of the down-cores used in this study are shown as follows: (1) the age models for those cores with planktonic foraminiferal AMS ^{14}C records (Fig. S1) are established by updated CALIB 7.0 program with the Marine 13 calibration data set [Reimer et al., 2013]. The surface reservoir age (R) in the SCS is assigned to be ~460 yrs for the Holocene and ~760 yrs for the LGM based on the recent marine ^{14}C reservoir age simulations [Butzin et al., 2017]; (2) for the cores without foraminiferal ^{14}C dating (Fig. S2), the ages of *C. wuellerstorfi* $\delta^{18}O$ records were determined by correlating to the regional benthic $\delta^{18}O$ stack of North Pacific intermediate sites by Stern and Lisiecki [2014], which was constructed by ^{14}C-dated records from North Pacific over the most recent deglaciation. Overall, the late Holocene sections were identified by minor $\delta^{18}O$ and $\delta^{13}C$ changes within the Holocene intervals or from radiocarbon dates. The LGM sections were identified by their highest $\delta^{18}O$ values of *C. wuellerstorfi* or from radiocarbon dates. (Fig. S1-S4).

Figures

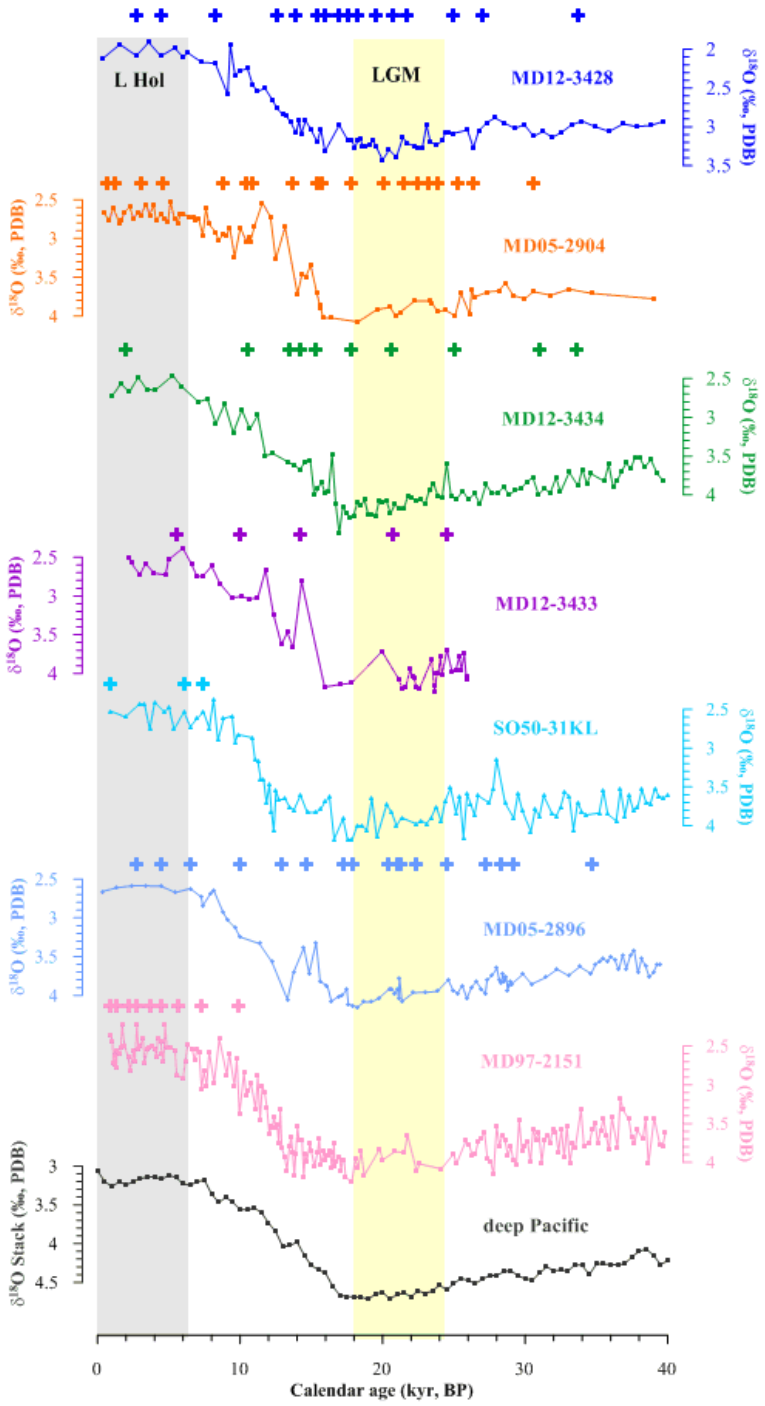

Figure S1: Age models based on *G. ruber* AMS ^{14}C records and *C. wuellerstorfi* δ^{18}O of Cores MD12-3428 (navy blue), MD05-2904 (orange line and signals), MD12-3434 (grass green), MD12-3433 (purple), SO50-31KL (light blue), MD05-2896 (pale blue), and MD97-2151(pink) in the SCS [Wei et al., 2006; Wan and Jian, 2014]. The crosses indicate the AMS^{14}C dating control points in these cores. The bottom δ^{18}O stack is the regional benthic δ^{18}O stack in the North Pacific [Stern and Lisiecki, 2014]. The light grey and orange bars show the intervals of the late Holocene (0-6 ky BP) and LGM (18-24 ky BP), respectively.

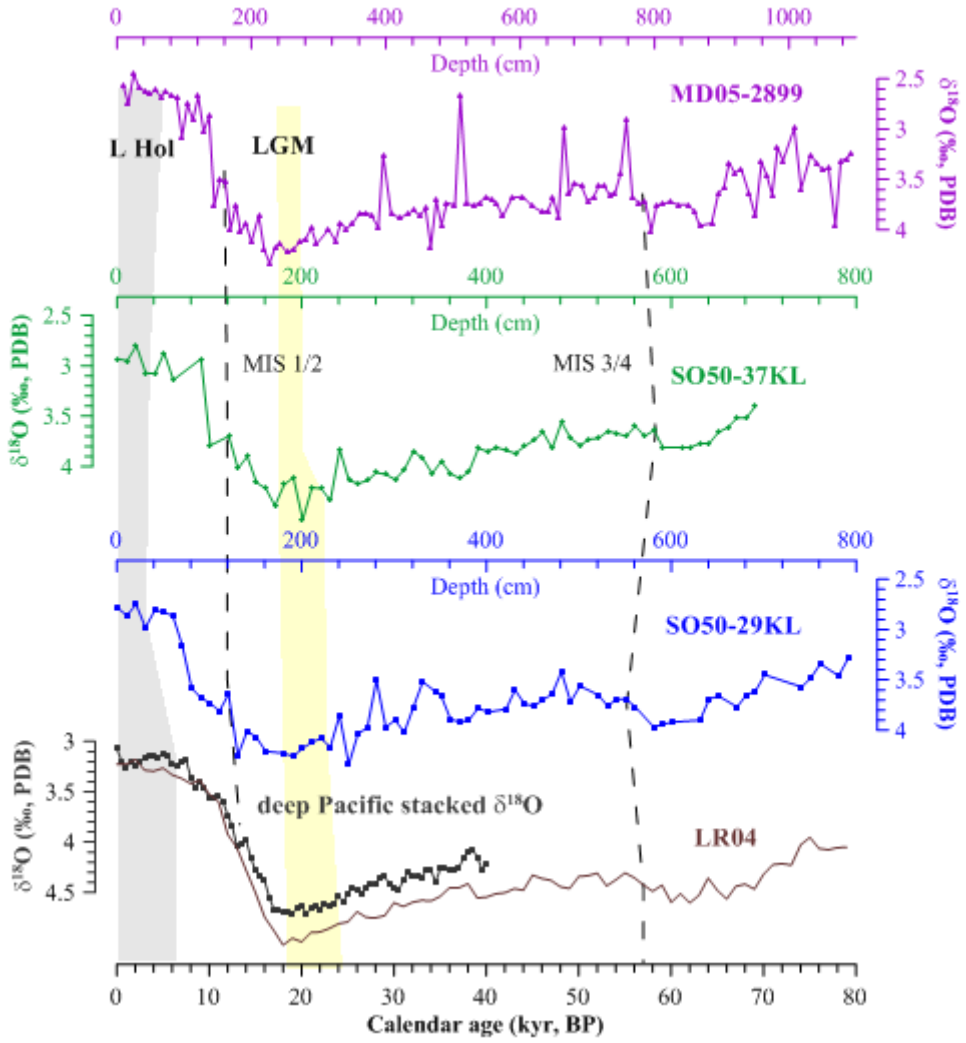

Figure S2: Determination of the late Holocene and LGM time slices for the *C. wuellerstorfi* $\delta^{18}O$ of Cores MD05-2899 (purple line and symbols), SO50-37KL (green), and SO50-29KL (dark blue) in the SCS [Qian, 1999]. The bottom benthic $\delta^{18}O$ reference curves come from the regional (the North Pacific) and global LR04 stacks, respectively [Stern and Lisiecki, 2014; Lisiecki and Raymo, 2005]. The light grey and orange polygons indicate general constraints on the intervals of the late Holocene and LGM, respectively. The dashed lines represent the rapid shifts of $\delta^{18}O$ on the MIS 1/2 and 3/4 boundaries as age control points.

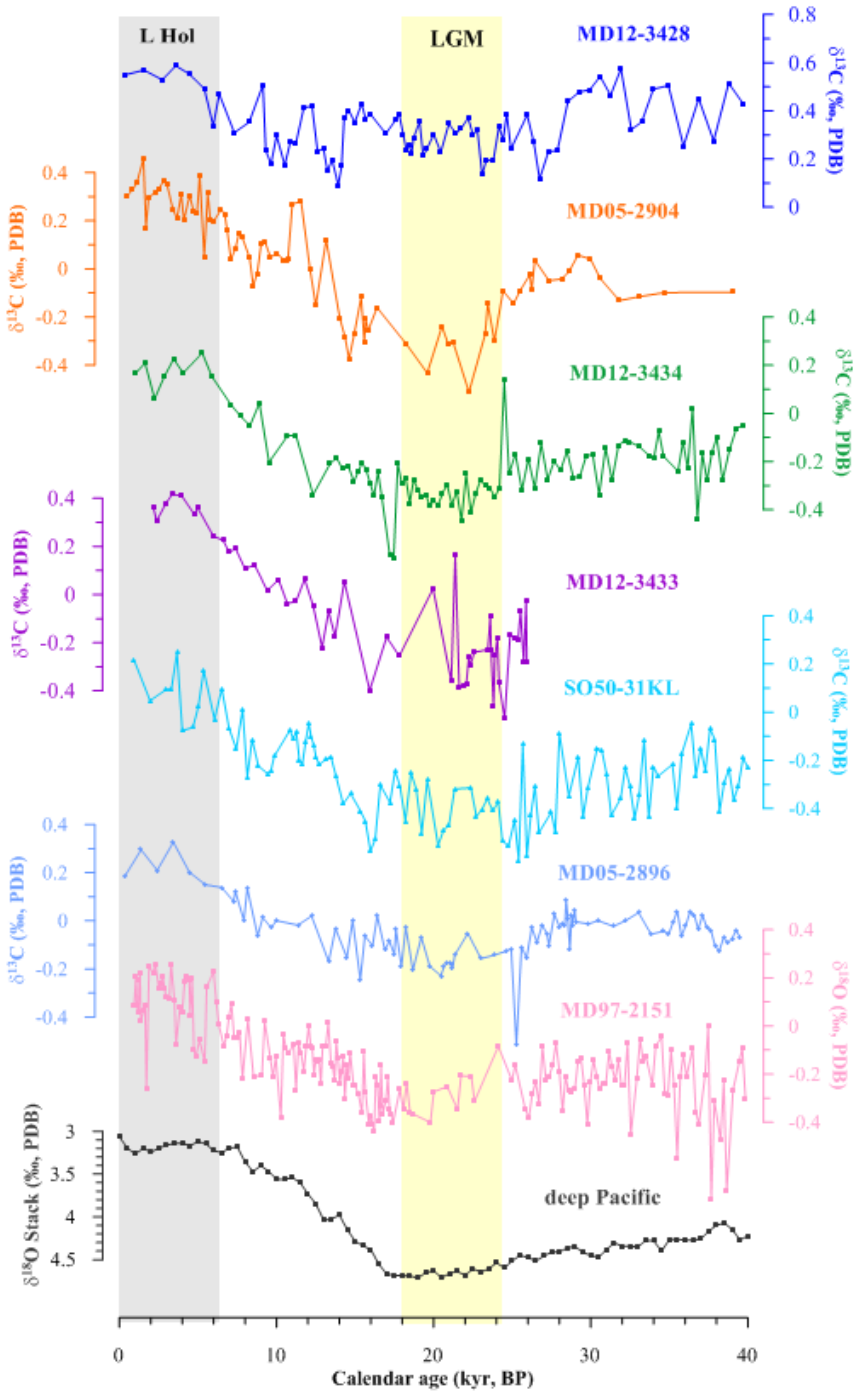

Figure S3: *C. wuellerstorfi* $\delta^{13}C$ records from Cores MD12-3428 (navy blue), MD05-2904 (orange line and signals), MD12-3434 (grass green), MD12-3433 (purple), SO50-31KL (light blue), MD05-2896 (pale blue), and MD97-2151(pink) in the SCS [Wei et al., 2006; Wan and Jian, 2014]. The bottom $\delta^{18}O$ stack is the regional benthic $\delta^{18}O$ stack in the North Pacific [Stern and Lisiecki, 2014]. The light grey and orange bars show the intervals of the late Holocene (0-6 ky BP) and LGM (18-24 ky BP), respectively.

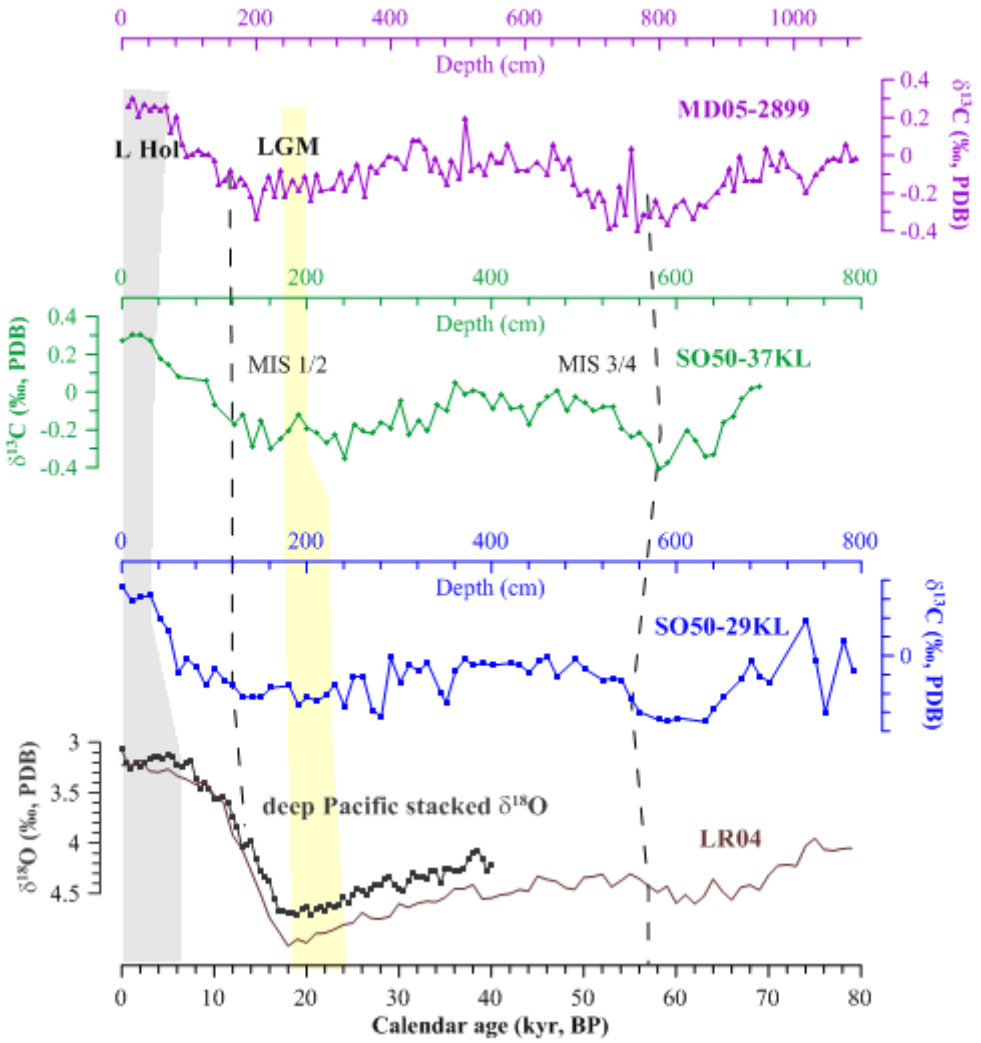

Figure S4: *C. wuellerstorfi* $\delta^{13}C$ records from Cores MD05-2899 (purple line and symbols), SO50-37KL (green), and SO50-29KL (dark blue) in the SCS [Qian, 1999]. The bottom benthic $\delta^{18}O$ reference curves come from the regional (the North Pacific) and global LR04 stacks, respectively [Stern and Lisiecki, 2014; Lisiecki and Raymo, 2005]. The light grey and orange polygons indicate general constraints on the intervals of the late Holocene and LGM, respectively. The dashed lines represent the rapid shifts of $\delta^{18}O$ on the MIS 1/2 and 3/4 boundaries.

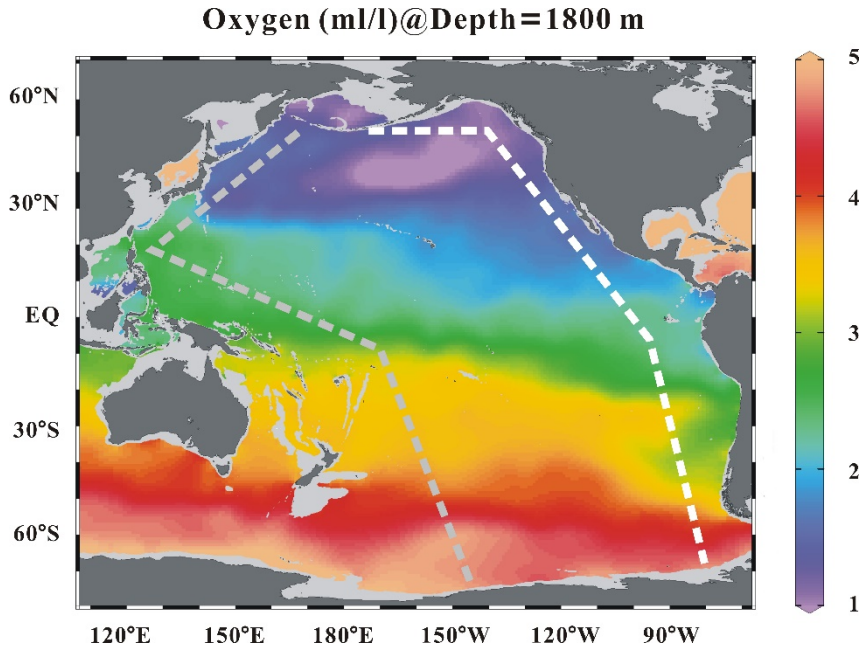

Figure S5: The selected transects in the western (grey broken line) and eastern (white broken line) Pacific. The colors of oceanic background show oxygen concentration at depth of 1800 m based on World Ocean Atlas 2013 [Garcia et al., 2013].

References

Bostock, H. C., Barrows T. T., Carter L., et al., 2013. A review of the Australian–New Zealand sector of the Southern Ocean over the last 30 ka (Aus-INTIMATE project). *Quat. Sci. Rev.*, 74, 35-57.

Butzin, M., Köhler P. & Lohmann G., 2017. Marine radiocarbon reservoir age simulations for the past 50,000 years. *Geophys. Res. Lett.*, 44, 8473-8480.

Cheng, X., Huang, B., Jian, Z., et al., 2005. Foraminiferal isotopic evidence for monsoonal activity in the South China Sea: a present-LGM comparison. *Mar. Micropaleontol*. 54, 125-139.

Garcia, H. E., Locarnini, R. A., Boyer, T. P., et al., 2014. World Ocean Atlas 2013, Volume 3: Dissolved Oxygen, Apparent Oxygen Utilization, and Oxygen Saturation. S. Levitus, Ed., A. Mishonov Technical Ed.; *NOAA Atlas NESDIS* 75, 27 pp.

Herguera, J. C., Jansen E. & Berger W. H., 1992. Evidence for a bathyal front at 2000-m depth in the glacial Pacific, based on a depth transect on Ontong Java Plateau. *Paleoceanography*, 7, 273-288.

Huang, C.-Y., Wu, S.-F., Zhao, M., et al., 1997. Surface ocean and monsoon climate variability in the South China Sea since the last glaciation. Mar. Micropaleontol. 32, 71-94.

Jian, Z. & Wang, L., 1997. Late Quaternary benthic foraminifera and deep-water paleoceanography in

the South China Sea. *Mar. Micropaleontol*. 32, 127-154.

Lisiecki, L.E., Raymo, M.E., 2005. A Pliocene-Pleistocene stack of 57 globally distributed benthic $\delta^{18}O$ records. *Paleoceanography* 20, PA1003.

Matsumoto, K., Oba T., Lynch-Stieglitz J. & Yamamoto H., 2002. Interior hydrography and circulation of the glacial Pacific Ocean. *Quat. Sci. Rev.*, 21, 1693-1704.

Oppo, D.W. & Fairbanks, R.G., 1987. Variability in the deep and intermediate water circulation of the Atlantic Ocean during the past 25,000 years: Northern Hemisphere modulation of the Southern Ocean. *Earth Planet. Sci. Lett.* 86, 1-15.

Qian J., 1999. Paleoceanography for the late Quaternary in the South China Sea. *China Sci. Press*, Beijing, pp: 39-55 (in Chinese).

Reimer, P. J., Bard E., Bayliss A., Beck J. W., et al., 2013. IntCal13 and Marine13 radiocarbon age calibration curves 0–50,000 Years cal BP. *Radiocarbon*, 55, 1869-1887.

Schmidt, G.A., Bigg, G. R. & Rohling, E. J., 1999. "Global Seawater Oxygen-18 Database - v1.21" http://data.giss.nasa.gov/o18data/.

Stern, J.V. & Lisiecki, L.E., 2014. Termination 1 timing in radiocarbon-dated regional benthic $\delta^{18}O$ stacks. *Paleoceanography*, 2014PA002700.

Tian, J., Wang, P., Cheng, X., Li, Q., 2002. Astronomically tuned Plio–Pleistocene benthic $\delta^{18}O$ record from South China Sea and Atlantic–Pacific comparison. *Earth Planet. Sci. Lett*. 203, 1015-1029.

Wan, S. & Jian, Z., 2014. Deep water exchanges between the South China Sea and the Pacific since the last glacial period. *Paleoceanography*, 2013PA002578.

Wang, L., Sarnthein, M., Erlenkeuser, H., et al., 1999. East Asian monsoon climate during the Late Pleistocene: high-resolution sediment records from the South China Sea. *Mar. Geol.* 156, 245-284.

Wei, G.-J., Huang, C.-Y., Wang, C.-C., et al., 2006. High-resolution benthic foraminifer $\delta^{13}C$ records in the South China Sea during the last 150 ka. *Mar. Geol.* 232, 227-235.